Article

A Test of Sol–Gel Incorporation of Organic Compounds as Translucent, Marine Biofouling-Resistant Windows

Malcolm Dale Stokes

Marine Physical Laboratory, Scripps Institution of Oceanography, La Jolla, CA 92037, USA; dstokes@ucsd.edu

Abstract: Organic compounds, including antimicrobial agents azithromycin and hydrous allicin extracts, were sequestered in a silicate sol–gel matrix to function as a biofouling-resistant window for oceanographic instrumentation. The windows fabricated in this manner resisted the formation of microbial biofilms (the precursor to settlement of larger macro-fouling organisms) for up to a week and maintained low levels of fouling for 3 weeks, whereas bare glass substrates form biofilms within hours of seawater submersion. The technique shows promise for the construction of additional translucent solids and coatings using other environmentally friendly biocides.

Keywords: biofouling; sol–gel; biofilm

1. Introduction

Great efforts have been taken to mitigate the effects of fouling organisms on the vessels, structures and instrumentation used in the marine environment. For many decades, toxic paints and claddings have been applied to submerged objects to deter the settlement of marine organisms [1–4]. The potent heavy metals and organic derivatives containing arsenic, mercury or lead have been restricted due to their risks to the environment, and the very successful tributyltin self-polishing copolymer antifoulant paints (TBT) were globally banned from application in 2003 because of their negative effects on many marine species, even at extremely low concentrations, and the bioaccumulation of TBT in marine food chains [5–8].

Marine biofouling follows a complex, multi-step process [1,2,9]. In general, an initial coating of organic and inorganic molecules accumulates on fresh surfaces, governed by van der Waals and electrostatic forces and Brownian motion. Next, rapidly growing bacteria and single-cell diatoms colonize the altered surface. These microorganisms secrete extracellular polymeric substances that coat and anchor them to the substrate and, together with additional protozoa (the species depending on the environment), form a dynamic microbial biofilm. The formation of the biofilm assists in the entrapment of additional particles and the attraction of a succession of microorganisms, some of which use biofilms and their exudates as settlement cues. The final stages in fouling include the settlement of multicellular larvae and the growth of a complex community including primary producers (i.e., algae), grazers and decomposers and larger marine invertebrates (e.g., barnacles, mussels). A successful tactic to minimize extensive biofouling has been to try to prevent the formation of the precursor microbial films before the settlement of larger organisms and/or provide a pesticide that kills organisms upon settlement.

In the case of oceanographic instrumentation that requires transparent optical windows, the problems in combating biofouling are particularly acute [4,10]. The housed sensors may be particularly susceptible to changes in light transmission, and oceanographic devices are often deployed on platforms for autonomous operation for extended periods of time. So, an antifouling method must be used that not only prevents long-term fouling but also does not hinder optical transmission. In addition to manual (hand) cleaning, both passive and active approaches have been used. Some active systems include mechanical

wipers and copper shutters (e.g., [10]), electric field and UV radiation generation [11,12], ultrasonic vibration [13,14] and chlorine production via electrolysis [15]. Although they can be effective, active antifouling systems are power intensive, which can be problematic in small, autonomous instruments with a limited battery supply.

New passive antifouling treatments have been developed to replace the application of TBT compounds to instrumentation and structures. These include the shielding of critical optical windows by biofouling-resistant copper cages or locating the transparent components in close proximity to antifoulant-treated materials (e.g., [16,17]). These new materials have replaced TBT and other heavy metals with copper [18,19], silver and other metallic nanoparticles [20,21] or a burgeoning suite of organic and inorganic biocides [22–26], some of which can be based on natural algal toxins and bacterial antagonists [27]. These compounds are incorporated into new paints with bound biocides or ablative or leaching coatings (i.e., [16,28]) that can restrict biofilm production. In addition, there is a growing number of silicone elastomeric coatings and paints, and polySBMA coatings with a similar surface chemistry, that are slippery in response to attachment and restrict fouling (e.g., [29–31]). However, most of these coatings are opaque and cannot be placed directly on transparent sensor optics.

In this report, a transparent silicate sol–gel (xerogel) was used as a matrix to immobilize biocidal compounds that can be used as a passive fouling-resistant window for optical marine sensors. The sol–gel process is a low-temperature fabrication procedure utilizing the water hydrolyzation of a metal or metalloid alkoxide precursor, an acid catalyst and reaction/biocide compatible solvents. Hydrolysis creates silanol (Si–OH) that reacts to form siloxane polymers by colloidal condensation, forming a gel. The biocidal molecules are trapped by the growing siloxane chains, eventually forming a porous silicate matrix. The microstructure of the matrix can be modified by varying the solvent, water, alkoxide concentrations, the pH and the reaction temperature to achieve an optimum pore size to restrict leaching of the encapsulated compounds but still allow a functionally reactive surface chemistry. Because of these easily modified properties, their chemical inertness and transparency, sol–gel materials and their glass/ceramic composites are becoming commonplace in the production of a diverse series of biosensors, thin-film coatings, doped fibers, cast optical monoliths and other components (e.g., [32–34]). They can function either as fouling-release-promoting surfaces with microscopically slick properties that make it easy to dislodge fouling organisms by reducing the strength of attachment or as inherent fouling-resistant surfaces that inhibit settlement and biofilm growth (or combinations of both). Of the former xerogel fouling-release coatings, the sol–gel surface roughness and energy (hence, wettability and surface tension) can be tuned for weak boundary-layer bioadhesion (i.e., [35–43]). Additionally, xerogel-derived coatings resist biofilm formation by incorporating in situ biocides in various forms and activities, including sequestered catalysts for bromination, zwitterionic materials and encapsulation of proteins and whole-cell bacteria, among others [44–48]. During the past two decades, sol–gel-derived compounds have come to prominence as environmentally friendly and economically attractive alternatives to toxic, marine antifouling coatings and have garnered extensive review (e.g., [49–60]).

2. Materials and Methods

Potential biofouling-resistant compounds were sequestered within a sol–gel which is capable of immobilizing large molecules (i.e., enzyme molecules > 100 kDa in size) in the porous silicate matrix using a method partially adapted from Aylott et al. [61]. The porosity of the sol–gel can be modified by altering its water content during formulation. The formation of the sol–gel biomaterial was a two-step process in which a pH-buffered phosphate solution (50 mmol, pH = 6) containing the biofouling-resistant compounds was mixed with a hydrolyzed silicate precursor solution (pH = 2). The increase in pH after mixing initiated the condensation reaction, forming the sol–gel in approximately 5 min.

The sol–gel solution was poured into disk-shaped molds before it hardened and was then left to age for 4 days submerged in the buffer solution at 5 degrees Celsius. After aging,

the glassy disks were soaked for 15 min and then rinsed through a series of ethanol/distilled water mixtures (ratio of ethanol to H_2O of 25:75, 50:50, 75:25, 90:10, 99:1) before air-drying at 25 degrees Celsius. After completion, the translucent silicate disks were approximately 3 cm in diameter and 3 mm thick.

2.1. Sol–Gel Precursor

The sol–gel precursor was prepared in an ultrasonic bath (Branson B300, 34 kHz) to facilitate even mixing of the sol and contained 1.1 mL of deionized water, 1.8 mL of tetramethylorthosilicate (TMOS) and 30 μL of HCl (0.05 M). The mixture was sonicated for 30 min before adding the buffered biocide solutions in a 2:1 buffer-to-precursor ratio.

2.1.1. Antifouling Compounds

Several different compounds of known antimicrobial and/or pesticidal/germicidal function were suspended in the pH 6 phosphate buffer. The following were tested:

2.1.2. Permethrin

Permethrin (3-phenoxybenzyl (1RS) cis, trans-3-(2,2-dichlorovinyl)-2,2-dimethylcyclopropanecarboxylate) is a broad-spectrum pyrethroid neurotoxin well known to be highly toxic to marine vertebrate and invertebrate life [62–64] and is also known to inhibit microbial growth [63]. In the samples tested here, 150 μL of permethrin was added to 2000 μL of the phosphate buffer solution and mixed by stirring.

2.1.3. DEET

DEET (N,N-diethyl-3-methylbenzamide) is a common insecticide and repellent known to alter the function of certain invertebrate olfactory receptor neurons and inhibit the activity of the critical nervous system enzyme acetylcholinesterase [65–67]. Because 100% DEET is an immiscible substance, 150 μL of DEET was added to 2000 μL of the phosphate buffer solution and mixed by sonification for 30 min to produce a hydrocolloidal emulsion and then immediately mixed with the sol–gel precursor to enable encapsulation in the silicate matrix before coalescence of the DEET microdroplets.

2.1.4. Azithromycin

Azithromycin (2R,3S,4R,5R,8R,10R,11R,12S,13S,14R)-2-ethyl-3,4,10-trihydroxy-3,5,6,8,10,12, 14-heptamethyl-15-oxo-11-{[3,4,6-trideoxy-3-(dimethylamino)-β-D-xylo-hexopyranosyl]oxy}-1-oxa-6-azacyclopentadec-13-yl 2,6-dideoxy-3-C-methyl-3-O-methyl-α-L-ribo-hexopyranoside) is a broad-spectrum macrolide antibiotic that inhibits protein synthesis by binding with the bacterial ribosome [68,69]. A 0.03 g amount of azithromycin in powdered form was stirred into 1000 μL of ethanol, then mixed with 2000 μL of buffer solution followed by sonification for 5 min.

2.1.5. Allicin

The allicin extracts (including diallyl thiosulfinate; 2-propene-1-sulfinothioic acid, S-2-propenyl ester) used in this study contain some of the many organosulfate compounds derived from garlic plant (*Allium sativum*) homogenate. These compounds are well known for their antimicrobial properties [70], acting as cell growth inhibitors [71] and blocking cellular quorum sensing [72].

The extraction process used here followed the ultrasound-assisted method of Kimbaris et al. [73]. Samples of fresh garlic cloves weighing 100 g were homogenized with 30 mL of deionized H_2O in a blender and then the homogenate was distilled in either deionized H_2O or ethanol as a solvent at 25 degrees Celsius. Approximately 500 mL of homogenate and 100 mL of solvent were then sonicated in a flask for 30 min in an ultrasonic bath (Branson B300, 34 kHz transducer). After sonication, the supernatant was rinsed with 25 mL of saturated NaCL solution and vacuum-filtered to remove precipitates and residues. Although allicin is the principal active component remaining in the supernatants

after extraction, other thiosulfate compounds are undoubtedly present in trace amounts including diallyl, allyl methyl and dimethyl mono- to hexasulfides [73].

2.2. Spectral Light Transmission

The spectral transmission properties of the sol–gels from 340 to 900 nm wavelength were examined using a spectrophotometer (Milton Roy Spectronic 20). For ease in handling, sol–gel solutions were mixed directly within the 2.5 mL plastic cuvettes used for measurement in the spectrophotometer. The % light transmission of each sol–gel sample at each wavelength was normalized to 100% transmission in an empty cuvette.

2.3. Antifouling Assessment

The sol–gel disks (10 replicates) were clamped by their edges in an acrylic jig that held their flat sides exposed and were then hung in the seawater intake channel at the end of the Scripps Institution of Oceanography (SIO) pier. This enclosed channel, located downstream of the primary seawater supply pumps for SIO, provides a continuous stream of seawater with suspended microorganisms and nutrients that flows to the sand filter system and secondary pumps that then provide filtered seawater to SIO and the Birch Aquarium. The seawater channel provides a controlled test location protected from the turbulent surf zone adjacent to the pier and prevents damage to the disks from hydrodynamic forces and sand scour. In addition to the sol–gel disks, untreated glass microscope slides were clamped in the jigs alongside the sol–gels to serve as a control. The channel is not an exact analog of shallow oceanic conditions (it has a near-continuous unidirectional current and is partially covered, and, therefore, dark, and larger (>1 cm), potentially biofouling organisms are removed by coarse mesh screens at the primary pump intakes); however, there is enough biofouling in the channel to require approximately bi-monthly cleaning to prevent flow restrictions due to the settlement of secondary biofouling organisms (i.e., marine invertebrate larvae, algae, etc.) that attach to biofilm-coated channel walls.

The growth of microbial biofilms on the disks and slides was monitored for 3 weeks at approximately daily intervals (3 times during the last week). Biofilm growth on the samples was estimated by measuring the transmission of light through each disk using a simple transmissometer consisting of an LED light (6500 K color temperature) and thermally stable power source, collimator optics (Thorlabs), an amplified photodiode (Hamamatsu S1087, peak sensitivity 560 nm) with stable voltage reference and collecting optics (Thorlabs). The optical components and sample holding jig were all enclosed in a light-proof box with a fixed pathway of light transmission (40 mm pathlength). Output from the collimator imaged almost the entire surface of the sample disk and provided an average measure of transmitted light intensity.

When making a measurement, the disks were quickly removed from the seawater jig and placed in the transmissometer, and the photodiode output voltage was recorded. Heterogeneity in photodiode output across the sample disk was measured by first normalizing the voltage signal with a standard, clean glass slide and then taking 5 separate readings of each disk rotated slightly in the jig. The amplified voltage from the photodiode provided a measurement of the absorption of light by the growing microbes and was normalized to the voltage output at 100% transmission through the sterile disks at the start of the test. At twice-weekly intervals, some of the disks were examined with a stereomicroscope to verify that microbial films were indeed growing and that the light extinction being measured was primarily the result of biofilm formation and not the result of inorganic surface particle contamination. It should be noted that the methodology and experiment controls followed herein did not preclude the potential role of chemical leaching, discoloration during aging or other unknown factors that could cause changes to the light transmission stability of the sample disks over time.

3. Results

As shown in Figure 1, the sol–gel disk blank (without antifouling compounds added) had light transmission properties similar to common soda–lime float glass (window glass), with decreased transmission outside the visible wavelengths (<400 nm, >700 nm). The slightly lower transmission of the sol–gel may be due to microbubbles present in the mixed solutions and trapped in the solidified material that would not be present in float glass.
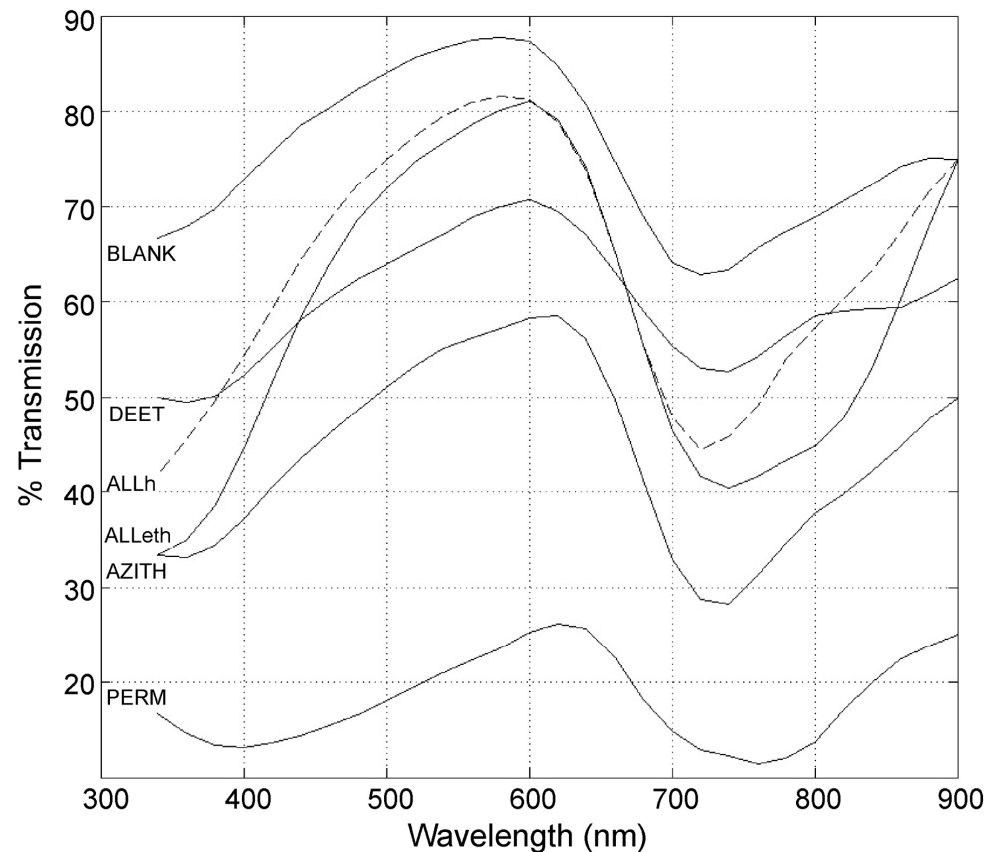

Figure 1. Spectral transmission properties of the sol–gel coatings from 300 to 900 nm wavelength. The transmissions are normalized to 100% transmission measured through an empty sampling cuvette. Curves labels indicate the sol–gel immobilized agents: DEET, ALLh (allicin H_2O extract), ALLeth (allicin ethanol extract), AZITH (azithromycin), PERM (permethrin). BLANK indicates transmission through the sol–gel material only.

The sol–gel materials containing the antifouling compounds showed lower light transmission at all wavelengths but retained peak transmission at approximately 600 nm. The sol–gel containing permethrin was the most opaque and showed a milky translucency. The sol–gels containing the H_2O- and ethanol-extracted allicin compounds showed the fewest transmission losses (although transparent, they retained a slight yellow tint to the eye, as expected with their narrower transmission spectrum with 600 nm peak).

When immersed in seawater, the bare glass slides immediately began to be covered in a microbial film (Figure 2). After 2 weeks, broad-band white light transmission through the glass had dropped approximately 18%. After this time, further reductions in transmission were not as detectable because the thickening biofilms began to continuously slough off in sections rather than remaining fixed to the substrate and further blocking light transmission.

The sol–gel disks with trapped antifouling agents all showed greater light transmission over time and resistance to microbial biofilm growth. The DEET and allicin ethanol extractions showed biofilm growth after two days and greater light transmission than the glass slides after 2 weeks (about 10% transmission loss). The DEET treatment was

terminated after 13 days when the fixture holding the disks was damaged and disrupted the growth of the microbial films.
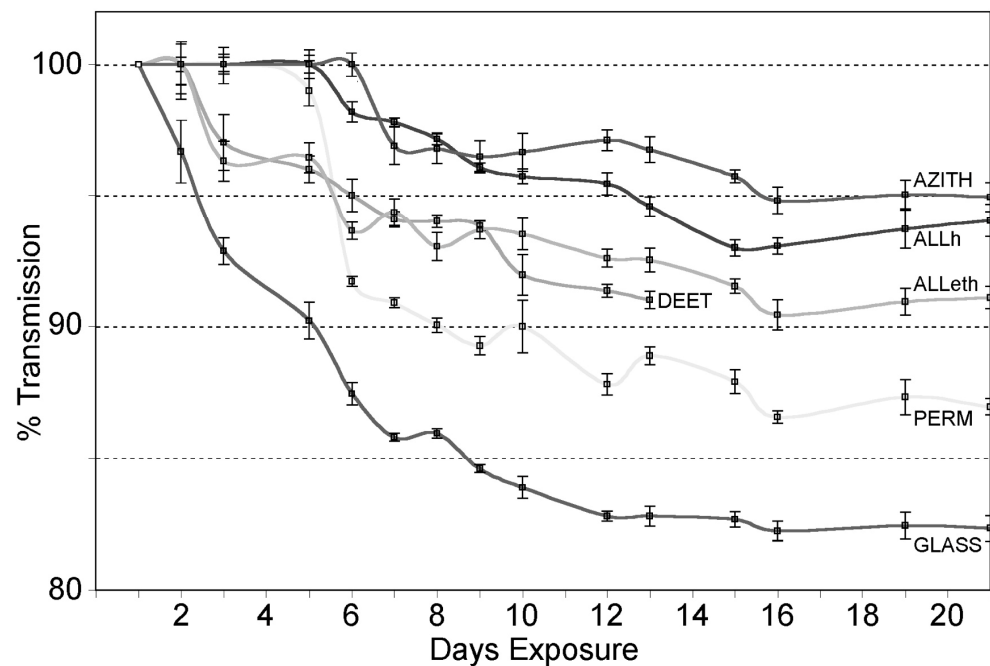

Figure 2. Percent light transmission over time. Light transmission in percent (mean ± S.D) through (*n* = 10) sol–gel disks with immobilized antifouling agents as in Figure 1. Transmission LED light source, 6500 K. Test substrates were bathed in running seawater at the end of the SIO pier for 3 weeks. Data are normalized to 100% transmission at the start of the treatment period. The curve labeled GLASS shows non-treated glass microscope slides suspended alongside the sol–gel disks. The DEET treatment was terminated when the fixture holding the DEET sol–gel disks was damaged.

The permethrin-containing sol–gels showed no light transmission loss or biofilm fouling after 5 days but then showed rapid microbial film growth. After 3 weeks, the mean light transmission through the sol–gel had decreased approximately 14%.

The allicin H$_2$O-extraction-treated sol–gels showed minimal biofilm fouling after 6 days, then slowly increasing light transmission losses. After 3 weeks, mean light transmission had decreased approximately 6% from that at the start of the trial.

The azithromycin-containing sol–gels showed minimal biofilm growth and minimal light transmission losses after 7 days of exposure. After 3 weeks, mean light transmission had decreased approximately 5% due to the gradual growth of microbial films on the disk surface.

4. Discussion

Biofouling of surfaces is a ubiquitous problem in the marine environment. For small oceanographic instruments, particularly those with components that require clear optical transmission pathways between sensors and the surrounding water, fouling organisms can quickly decrease the quality of their measured data. For power-limited optical devices, an ideal antifouling protection scheme is a passive protective coating that limits the creation of microbial biofilms (and then subsequent organism settlement) and that can be applied directly to the sensor window. This approach, used in conjunction with the additional protection offered by adjacent copper shielding and the use of other highly effective but opaque antifouling coatings on the instrument housing, would allow long-term deployments of oceanographic devices with lower maintenance and battery demands.

The sol–gel composite material tested here could be used as a biofilm-resistant window to slow the formation of biofilms. For instance, the windows fabricated incorporating

the allicin and azithromycin extracts showed little biofilm contamination after a week of submersion, whereas bare glass showed biofilm production in a matter of hours. Additionally, unlike other transparent coatings, such as superhydrophilic and other non-stick nanosurfaces (e.g., [73]), an entire window fabricated from a sol–gel composite may be more robust to surface damage and may remain biocidal longer than other thin, leaching antimicrobial coatings [24]. Fabricated as a secondary, sacrificial protective shield, the biocidal sol–gel window could be mechanically positioned exterior to a primary sensor window that is transparent and pressure resistant yet prone to biofouling. It should be noted that, although the antibiotic azithromycin has proved an effective biofilm retardant, widespread use as such is not condoned herein as it may promote the development of antibiotic resistance to this useful medical agent via potential leaching and mechanical ablation of the antibiotic from the sol–gel into the environment.

The sol–gel composite windows were only tested with respect to their prevention of the creation of biofilms because they were deployed in a seawater channel that provides less exposure to large, secondary settling macro-organisms such as barnacles and mussels than would exist if they were deployed directly in the ocean. All the composite materials showed much slower microbial growth than on a bare glass substrate, and, even after 3 weeks of submersion, the accumulated growth on the composites never approached the thick microbial films formed (and sloughing off) the bare glass. Because biofilm formation is an early, critical step in the formation of a complete fouling community, it is assumed that restricting biofilm formation slows the settlement of larger multicellular organisms and increases the usable deployment period of optical instrumentation. It must be noted that biofouling in the ocean is a complex and dynamic process and that some larger fouling organisms may not require the presence of a biofilm for a settlement cue and "Biofouling development on a surface is the net result of several physical, chemical and biological factors: temperature, conductivity, pH, dissolved oxygen content, organic material content; hydrodynamic conditions; location, season, light and consequently depth" [4]. A single, complete antifouling protection scheme is probably impossible.

A composite material containing encapsulated allicin compounds is particularly promising because these are naturally occurring and environmentally safe molecules displaying powerful antimicrobial properties (i.e., [70]). The sol–gel encapsulation process could conceivably be used in a similar fashion to formulate composite glass materials containing other naturally occurring compounds with antibiotic and bio-deterrent properties such as capsaicin, piperine and allyl isothiocyanate. It is also conceivable that many different compounds of similar molecular size could be combined in a single composite sol–gel to provide broad-spectrum biofouling resistance that first slows biofilm formation and then acts as a biocide/deterrent to later multicellular fouling organisms. The combination of multiple quorum-blocking and compatible biocidal compounds into the one sol–gel silicate matrix is currently under active study. Ideally, an antifouling window of hybrid design incorporating environmentally safe biocidal molecules for in situ resistance to biofilm formation and organism settlement, as well as the tunable surface wettability and roughness possible with sol–gels to reduce adhesion, provides close to an ideal passive antifouling solution for marine instrumentation.

Conflicts of Interest: The author declares no conflict of interest.

References

1. Yebra, D.M.; Kiil, S.; Dam-Johansen, K. Antifouling technology—Past, present and future steps towards efficient and environmentally friendly antifouling coatings. *Prog. Org. Coat.* **2004**, *50*, 75–104. [CrossRef]
2. Chambers, L.D.; Stokes, K.R.; Walsh, F.C.; Wood, R.J. Modern approaches to marine antifouling coatings. *Surf. Coat. Technol.* **2006**, *201*, 3642–3652. [CrossRef]
3. Delgado, A.; Briciu-Burghina, C.; Regan, F. Antifouling strategies for sensors used in water monitoring: Review and future perspectives. *Sensors* **2021**, *21*, 389. [CrossRef]
4. Delauney, L.; Compère, C.; Lehaitre, M. Biofouling protection for marine environmental sensors. *Ocean. Sci.* **2009**, *6*, 503–511. [CrossRef]
5. Batley, G.E.; Scammell, M.S.; Brockbank, C.I. The impact of the banning of tributyltin-based antifouling paints on the Sydney rock oyster, *Saccostrea commercialis*. *Sci. Total Environ.* **1992**, *122*, 301–314. [CrossRef] [PubMed]
6. Thomas, K.; Raymond, K.; Chadwick, J.; Waldock, M. The effects of short-term changes in environmental parameters on the release of biocides from antifouling coatings: Cuprous oxide and tributyltin. *Appl. Organomet. Chem.* **1999**, *13*, 453–460. [CrossRef]
7. Thomas, K.V.; Fileman, T.W.; Readman, J.W.; Waldock, M.J. Antifouling paint booster biocides in the UK coastal environment and potential risks of biological effects. *Mar. Pollut. Bull.* **2001**, *42*, 677–688. [CrossRef]
8. Almeida, E.; Diamantino, T.C.; de Sousa, O. Marine paints: The particular case of antifouling paints. *Prog. Org. Coat.* **2007**, *59*, 2–10. [CrossRef]
9. Lejars, M.; Margaillan, A.; Bressy, C. Fouling release coatings: A nontoxic alternative to biocidal antifouling coatings. *Chem. Rev.* **2012**, *112*, 4347–4390. [CrossRef]
10. Manov, D.V.; Chang, G.C.; Dickey, T.D. Methods for reducing biofouling of moored optical sensors. *J. Atmos. Ocean. Technol.* **2004**, *21*, 958–968. [CrossRef]
11. Block, R.; Leipold, F.; Lebahn, K.; May, H.; Schoenbach, K.H.; Royer, T.C.; Atkinson, L.P.; Wullschleger, T. Pulsed electric field based antifouling method for salinometers. In Proceedings of the 28th IEEE International Conference on Plasma Science and 13th IEEE International Pulsed Power Conference, Las Vegas, NV, USA, 17–22 June 2001.
12. Patil, J.S.; Kimoto, H.; Kimoto, T.; Saino, T. Ultraviolet radiation (UV-C): A potential tool for the control of biofouling on marine optical instruments. *Biofouling* **2007**, *23*, 215–230. [CrossRef]
13. Rahmoune, M.; Latour, M. Application of mechanical waves induced by piezofilms to marine fouling protection of oceanographic sensors. *Smart Mater. Struct.* **1995**, *4*, 195. [CrossRef]
14. Nogué, M.G.; Akbarsyah, I.J.; Bolhuis-Versteeg, L.A.; Lammertink, R.G.; Wessling, M. Vibrating polymeric microsieves: Antifouling strategies for microfiltration. *J. Membr. Sci.* **2006**, *285*, 323–333. [CrossRef]
15. Delauney, L.; Compère, C. An example: Biofouling protection for marine environmental sensors by local chlorination. In *Marine and Industrial Biofouling*; Springer: Berlin/Heidelberg, Germany, 2009.
16. Strahle, W.J.; Perez, C.L.; Martini, M.A. Antifouling leaching technique for optical lenses. In Proceedings of the IEEE OCEANS'94, Brest, France, 13–16 September 1994.
17. Kerr, A.; Smith, M.J.; Cowling, M.J. Optimising optical port size on underwater marine instruments to maximise biofouling resistance. *Mater. Des.* **2003**, *24*, 247–253. [CrossRef]
18. Srinivasan, M.; Swain, G.W. Managing the use of copper-based antifouling paints. *Environ. Manag.* **2007**, *39*, 423–441. [CrossRef]
19. Anyaogu, K.C.; Fedorov, A.V.; Neckers, D.C. Synthesis, characterization, and antifouling potential of functionalized copper nanoparticles. *Langmuir* **2008**, *24*, 4340–4346. [CrossRef]
20. Kawashita, M.; Tsuneyama, S.; Miyaji, F.; Kokubo, T.; Kozuka, H.; Yamamoto, K. Antibacterial silver-containing silica glass prepared by sol–gel method. *Biomaterials* **2000**, *21*, 393–398. [CrossRef]
21. Dineshram, R.; Subasri, R.; Somaraju, K.R.; Jayaraj, K.; Vedaprakash, L.; Ratnam, K.; Joshi, S.V.; Venkatesan, R. Biofouling studies on nanoparticle-based metal oxide coatings on glass coupons exposed to marine environment. *Colloids Surf. B Biointerfaces* **2009**, *74*, 75–83. [CrossRef]
22. Meinema, H.; Rentrop, C.; Breur, H.; Ferrari, J. Development and screening of organic inorganic hybrid coatings with antifouling properties for application on optical underwater instruments. In Proceedings of the 1st International Conference on Coatings on Glass-ICCG, Saarbrucken, Germany, 27–31 October 1997.
23. Smith, M.J.; Adam, G.; Duncan, H.J.; Cowling, M.J. The effects of cationic surfactants on marine biofilm growth on hydrogels. *Estuar. Coast. Shelf Sci.* **2002**, *55*, 361–367. [CrossRef]
24. Zhang, M.; Cabane, E.; Claverie, J. Transparent antifouling coatings via nanoencapsulation of a biocide. *J. Appl. Polym. Sci.* **2007**, *105*, 3826–3833. [CrossRef]
25. Booth, C.; Wheeler, P.; Hancock, J.; Ximenes, R.; Patterson, D.E. Optical behavior of antibiofouling additives in environment-friendly coverglass materials for bio-sensors and solar panels. *Polym. Adv. Technol.* **2009**, *20*, 626–630. [CrossRef]
26. Olsen, S.M.; Pedersen, L.T.; Hermann, M.H.; Kiil, S.; Dam-Johansen, K. Inorganic precursor peroxides for antifouling coatings. *J. Coat. Technol. Res.* **2009**, *6*, 187–189. [CrossRef]
27. Bhattarai, H.D.; Lee, Y.K.; Cho, K.H.; Lee, H.K.; Shin, H.W. The study of antagonistic interactions among pelagic bacteria: A promising way to coin environmentally friendly antifouling compounds. *Hydrobiologia* **2006**, *568*, 417–423. [CrossRef]
28. Strahle, W.J.; Hotchkiss, F.S.; Martini, M.A. Field results of antifouling techniques for optical instruments. In Proceedings of the IEEE OCEANS'98, Nice, France, 28 September–1 October 1998.

29. Hu, P.; Xie, Q.; Ma, C.; Zhang, G. Silicone-based fouling-release coatings for marine antifouling. *Langmuir* **2020**, *36*, 2170–2183. [CrossRef] [PubMed]

30. Cooper, S.P.; Finlay, J.A.; Cone, G.; Callow, M.E.; Callow, J.A.; Brennan, A.B. Engineered antifouling microtopographies: Kinetic analysis of the attachment of zoospores of the green alga Ulva to silicone elastomers. *Biofouling* **2011**, *27*, 881–892. [CrossRef] [PubMed]

31. Kaffashi, A.; Jannesari, A.; Ranjbar, Z. Silicone fouling-release coatings: Effects of the molecular weight of poly (dimethylsiloxane) and tetraethyl orthosilicate on the magnitude of pseudobarnacle adhesion strength. *Biofouling* **2012**, *28*, 729–741. [CrossRef] [PubMed]

32. Wang, J. Sol-gel materials for electrochemical biosensors. *Anal. Chim. Acta* **1999**, *399*, 21–27. [CrossRef]

33. Akesso, L.; Pettitt, M.E.; Callow, J.A.; Callow, M.E.; Stallard, J.; Teer, D.; Liu, C.; Wang, S.; Zhao, Q.; D'Souza, F.; et al. The potential of nano-structured silicon oxide type coatings deposited by PACVD for control of aquatic biofouling. *Biofouling* **2009**, *25*, 55–67. [CrossRef]

34. Wang, T.; Huang, L.; Liu, Y.; Li, X.; Liu, C.; Handschuh-Wang, S.; Xu, Y.; Zhao, Y.; Tang, Y. Robust Biomimetic Hierarchical Diamond Architecture with a Self-Cleaning, Antibacterial, and Antibiofouling Surface. *ACS Appl. Mater. Interfaces* **2020**, *12*, 24432–24441. [CrossRef]

35. Tang, Y.; Finlay, J.A.; Kowalke, G.L.; Meyer, A.E.; Bright, F.V.; Callow, M.E.; Callow, J.A.; Wendt, D.E.; Detty, M.R. Hybrid xerogel films as novel coatings for antifouling and fouling release. *Biofouling* **2005**, *21*, 59–71. [CrossRef]

36. Genzer, J.; Efimenko, K. Recent developments in superhydrophobic surfaces and their relevance to marine fouling: A review. *Biofouling* **2006**, *22*, 339–360. [CrossRef]

37. Richards, C.; Briciu-Burghina, C.; Jacobs, M.R.; Barrett, A.; Regan, F. Assessment of antifouling potential of novel transparent sol gel coatings for application in the marine environment. *Molecules* **2019**, *24*, 2983. [CrossRef]

38. Zada, T.; Reches, M.; Mandler, D. Antifouling and antimicrobial coatings based on sol–gel films. *J. Sol-Gel Sci. Technol.* **2020**, *95*, 609–619. [CrossRef]

39. Scandura, G.; Ciriminna, R.; Ozer, L.Y.; Meneguzzo, F.; Palmisano, G.; Pagliaro, M. Antifouling and photocatalytic antibacterial activity of the AquaSun coating in seawater and related media. *ACS Omega* **2017**, *2*, 7568–7575. [CrossRef] [PubMed]

40. Wanka, R.; Koc, J.; Clarke, J.; Hunsucker, K.Z.; Swain, G.W.; Aldred, N.; Finlay, J.A.; Clare, A.S.; Rosenhahn, A. Sol–gel-based hybrid materials as antifouling and fouling-release coatings for marine applications. *ACS Appl. Mater. Interfaces* **2020**, *12*, 53286–53296. [CrossRef]

41. Rosenhahn, A.; Schilp, S.; Kreuzer, H.J.; Grunze, M. The role of "inert" surface chemistry in marine biofouling prevention. *Phys. Chem. Chem. Phys.* **2010**, *12*, 4275–4286. [CrossRef]

42. Gunari, N.; Brewer, L.H.; Bennett, S.M.; Sokolova, A.; Kraut, N.D.; Finlay, J.A.; Meyer, A.E.; Walker, G.C.; Wendt, D.E.; Callow, M.E.; et al. The control of marine biofouling on xerogel surfaces with nanometer-scale topography. *Biofouling* **2011**, *27*, 137–149. [CrossRef]

43. Evariste, E.; Gatley, C.M.; Detty, M.R.; Callow, M.E.; Callow, J.A. The performance of aminoalkyl/fluorocarbon/hydrocarbon-modified xerogel coatings against the marine alga *Ectocarpus crouaniorum*: Relative roles of surface energy and charge. *Biofouling* **2013**, *29*, 171–184. [CrossRef]

44. Ferreira-Vançato, Y.C.; Dantas, F.M.; Fleury, B.G. Nanobiocides against marine biofouling. *Stud. Nat. Prod. Chem.* **2020**, *67*, 463–514.

45. Bennett, S.M.; Tang, Y.; McMaster, D.; Bright, F.V.; Detty, M.R. A xerogel-sequestered selenoxide catalyst for brominations with hydrogen peroxide and sodium bromide in an aqueous environment. *J. Org. Chem.* **2008**, *73*, 6849–6852. [CrossRef]

46. McMaster, D.M.; Bennett, S.M.; Tang, Y.; Finlay, J.A.; Kowalke, G.L.; Nedved, B.; Bright, F.V.; Callow, M.E.; Callow, J.A.; Wendt, D.E.; et al. Antifouling character of 'active' hybrid xerogel coatings with sequestered catalysts for the activation of hydrogen peroxide. *Biofouling* **2009**, *25*, 21–33. [CrossRef] [PubMed]

47. Jiang, S.; Cao, Z. Ultralow-fouling, functionalizable, and hydrolyzable zwitterionic materials and their derivatives for biological applications. *Adv. Mater.* **2010**, *22*, 920–932. [CrossRef] [PubMed]

48. Gatley-Montross, C.M.; Finlay, J.A.; Aldred, N.; Cassady, H.; Destino, J.F.; Orihuela, B.; Hickner, M.A.; Clare, A.S.; Rittschof, D.; Holm, E.R.; et al. Multivariate analysis of attachment of biofouling organisms in response to material surface characteristics. *Biointerphases* **2017**, *12*, 051003. [CrossRef]

49. Sfameni, S.; Rando, G.; Galletta, M.; Ielo, I.; Brucale, M.; De Leo, F.; Cardiano, P.; Cappello, S.; Visco, A.; Trovato, V.; et al. Design and Development of Fluorinated and Biocide-Free Sol–Gel Based Hybrid Functional Coatings for Anti-Biofouling/Foul-Release Activity. *Gels* **2022**, *8*, 538. [CrossRef]

50. Olsen, S.M.; Pedersen, L.T.; Laursen, M.H.; Kiil, S.; Dam-Johansen, K. Enzyme-based antifouling coatings: A review. *Biofouling* **2007**, *23*, 369–383. [CrossRef]

51. Regan, F.; Barrett, A.; Briciu-Burghina, C.; Sullivan, T. Antifouling studies and coating strategies for marine deployed structures. In Proceedings of the IEEE OCEANS'17, Aberdeen, Scotland, 19–22 June 2017.

52. Salta, M.; Wharton, J.A.; Stoodley, P.; Dennington, S.P.; Goodes, L.R.; Werwinski, S.; Mart, U.; Wood, R.J.; Stokes, K.R. Designing biomimetic antifouling surfaces. *Philos. Trans. R. Soc. A Math. Phys. Eng. Sci.* **2010**, *368*, 4729–4754. [CrossRef]

53. Banerjee, I.; Pangule, R.C.; Kane, R.S. Antifouling coatings: Recent developments in the design of surfaces that prevent fouling by proteins, bacteria, and marine organisms. *Adv. Mater.* **2011**, *23*, 690–718. [CrossRef]

54. Callow, J.A.; Callow, M.E. Trends in the development of environmentally friendly fouling-resistant marine coatings. *Nat. Commun.* **2011**, *2*, 244. [CrossRef]
55. Kirschner, C.M.; Brennan, A.B. Bio-inspired antifouling strategies. *Annu. Rev. Mater. Res.* **2012**, *42*, 211–229. [CrossRef]
56. Carve, M.; Scardino, A.; Shimeta, J. Effects of surface texture and interrelated properties on marine biofouling: A systematic review. *Biofouling* **2019**, *35*, 597–617. [CrossRef]
57. Sokolova, A.; Cilz, N.; Daniels, J.; Stafslien, S.J.; Brewer, L.H.; Wendt, D.E.; Bright, F.V.; Detty, M.R. A comparison of the antifouling/foul-release characteristics of non-biocidal xerogel and commercial coatings toward micro-and macrofouling organisms. *Biofouling* **2012**, *28*, 511–523. [CrossRef] [PubMed]
58. Detty, M.R.; Ciriminna, R.; Bright, F.V.; Pagliaro, M. Environmentally benign sol–gel antifouling and foul-releasing coatings. *Acc. Chem. Res.* **2014**, *47*, 678–687. [CrossRef] [PubMed]
59. Gittens, J.E.; Smith, T.J.; Suleiman, R.; Akid, R. Current and emerging environmentally-friendly systems for fouling control in the marine environment. *Biotechnol. Adv.* **2013**, *31*, 1738–1753. [CrossRef]
60. Aylott, J.; Richardson, D.; Russell, D. Optical biosensing of nitrate ions using a sol–gel immobilized nitrate reductase. *Analyst* **1997**, *122*, 77–80. [CrossRef]
61. Anderson, R.L. Toxicity of fenvalerate and permethrin to several nontarget aquatic invertebrates. *Environ. Entomol.* **1982**, *11*, 1251–1257. [CrossRef]
62. Coats, J.R.; Symonik, D.M.; Bradbury, S.P.; Dyer, S.D.; Timson, L.K.; Atchison, G.J. Toxicology of synthetic pyrethroids in aquatic organisms: An overview. *Environ. Toxicol. Chem. Int. J.* **1989**, *8*, 671–679. [CrossRef]
63. Sibley, P.K.; Kaushik, N.K. Toxicity of microencapsulated permethrin to selected nontarget aquatic invertebrates. *Arch. Environ. Contam. Toxicol.* **1991**, *20*, 168–176. [CrossRef]
64. Ditzen, M.; Pellegrino, M.; Vosshall, L.B. Insect odorant receptors are molecular targets of the insect repellent DEET. *Science* **2008**, *319*, 1838–1842. [CrossRef]
65. Syed, Z.; Leal, W.S. Mosquitoes smell and avoid the insect repellent DEET. *Proc. Natl. Acad. Sci. USA* **2008**, *105*, 13598–13603. [CrossRef]
66. Corbel, V.; Stankiewicz, M.; Pennetier, C.; Fournier, D.; Stojan, J.; Girard, E.; Dimitrov, M.; Molgó, J.; Hougard, J.M.; Lapied, B. Evidence for inhibition of cholinesterases in insect and mammalian nervous systems by the insect repellent deet. *BMC Biol.* **2009**, *7*, 47. [CrossRef]
67. Scheld, W.M.; Whitman, M.S.; Tunkel, A.R. Azithromycin and clarithromycin overview and comparison with erythromycin. *Infect. Control Hosp. Epidemiol.* **1992**, *13*, 357–368.
68. Luke, D.R.; Foulds, G.; Cohen, S.F.; Levy, B. Safety, toleration, and pharmacokinetics of intravenous azithromycin. *Antimicrob. Agents Chemother.* **1996**, *40*, 2577–2581. [CrossRef] [PubMed]
69. Harris, J.C.; Cottrell, S.L.; Plummer, S.; Lloyd, D. Antimicrobial properties of *Allium sativum* (garlic). *Appl. Microbiol. Biotechnol.* **2001**, *57*, 282–286. [CrossRef]
70. Ankri, S.; Mirelman, D. Antimicrobial properties of allicin from garlic. *Microbes Infect.* **1999**, *1*, 125–129. [CrossRef]
71. Bjarnsholt, T.; Jensen, P.Ø.; Rasmussen, T.B.; Christophersen, L.; Calum, H.; Hentzer, M.; Hougen, H.P.; Rygaard, J.; Moser, C.; Eberl, L.; et al. Garlic blocks quorum sensing and promotes rapid clearing of pulmonary *Pseudomonas aeruginosa* infections. *Microbiology* **2005**, *151*, 3873–3880. [CrossRef]
72. Kimbaris, A.C.; Siatis, N.G.; Daferera, D.J.; Tarantilis, P.A.; Pappas, C.S.; Polissiou, M.G. Comparison of distillation and ultrasound-assisted extraction methods for the isolation of sensitive aroma compounds from garlic (*Allium sativum*). *Ultrason. Sonochemistry* **2006**, *13*, 54–60. [CrossRef]
73. Patel, P.; Choi, C.K.; Meng, D.D. Superhydrophilic surfaces for antifogging and antifouling microfluidic devices. *JALA J. Assoc. Lab. Autom.* **2010**, *15*, 114–119. [CrossRef]